MOLECULAR AND CELLULAR BIOLOGY, Jan. 2008, p. 326–332 Vol. 28, No. 1
0270-7306/08/$08.00+0 doi:10.1128/MCB.01482-07

Prevention of Skin Tumorigenesis and Impairment of Epidermal Cell Proliferation by Targeted Aquaporin-3 Gene Disruption▽†

Mariko Hara-Chikuma and A. S. Verkman*

Departments of Medicine and Physiology, Cardiovascular Research Institute, University of California, San Francisco, California 94143

Received 16 August 2007/Returned for modification 26 September 2007/Accepted 12 October 2007

Aquaporin-3 (AQP3) is a water/glycerol-transporting protein expressed strongly at the plasma membranes of basal epidermal cells in skin. We found that human skin squamous cell carcinoma strongly overexpresses AQP3. A novel role for AQP3 in skin tumorigenesis was discovered using mice with targeted AQP3 gene disruption. We found that AQP3-null mice were remarkably resistant to the development of skin tumors following exposure to a tumor initiator and phorbol ester promoter. Though tumor initiator challenge produced comparable apoptotic responses in wild-type and AQP3-null mice, promoter-induced cell proliferation was greatly impaired in the AQP3-null epidermis. Reductions of epidermal cell glycerol, its metabolite glycerol-3-phosphate, and ATP were found in AQP3 deficiency without impairment of mitochondrial function. Glycerol supplementation corrected the reduced proliferation and ATP content in AQP3 deficiency, with cellular glycerol, ATP, and proliferative ability being closely correlated. Our data suggest involvement of AQP3-facilitated glycerol transport in epidermal cell proliferation and tumorigenesis by a novel mechanism implicating cellular glycerol as a key determinant of cellular ATP energy. AQP3 may thus be an important determinant in skin tumorigenesis and hence a novel target for tumor prevention and therapy.

Skin cancer, including malignant melanoma, basal cell carcinoma, and squamous cell carcinoma (SCC), is the most common human cancer and represents a major public health concern due to its high incidence and the medical costs, mortality, and cosmetic associated deformities. A multistage skin tumor model has been used extensively to study the cellular, biochemical, and genetic events linked to the initiation, promotion, and progression steps of skin carcinogenesis (14, 29). The tumor induction protocol involves treatment with a single dose of the tumor initiator 7,12-dimethylbenz[*a*]anthracene (DMBA) followed by multiple applications of the tumor promoter 12-*O*-tetradecanoylphorbol-13-acetate (TPA) (3, 30). This leads to the development of papillomas, which are benign neoplastic lesions consisting of hyperplastic keratinocytes and supporting stromal cells.

The aquaporins (AQPs) are a family of small, integral membrane proteins that transport water and in some cases small solutes, such as glycerol, termed aquaglyceroporins (AQPs 3, 7, and 9) (5, 27). Phenotype analysis of AQP knockout mice has revealed multiple roles for AQP-facilitated water transport in the urinary concentrating mechanism and in epithelial fluid secretion, brain edema, neural signal transduction, and cell migration (24, 28). In contrast, the aquaglyceroporins appear to be involved in metabolic pathways, such as adipose AQP7 in obesity (11, 12) and AQP9 in diabetes (22). The mechanisms underlying these phenomena were attributed to the glycerol-transporting function of aquaglyceroporins. In mammalian skin, AQP3 is expressed in plasma membranes of the basal epidermal cell layer (4, 16, 25). A human keratocarcinoma cell line has also been found to express AQP3 (20). AQP3-deficient mice have dry skin and delayed barrier recovery after removal of the stratum corneum (9, 16). We previously attributed these defects to the absence of AQP3-facilitated glycerol transport, resulting in reduced stratum corneum and epidermal cell glycerol content (9, 10).

Here, we report the remarkable observation that AQP3-deficient mice do not develop skin tumors in the established multistage skin tumor model described above. This study was motivated by the strong expression of AQP3 in the basal, proliferating layer of the normal mammalian epidermis and our finding in initial studies of greatly increased AQP3 expression throughout human skin tumors. A novel mechanism for the prevention of skin tumors by AQP3 gene disruption was discovered. We found reduced glycerol, glucose, and ATP levels in AQP3-deficient epidermal cells, which, together with additional studies, support a mechanism involving reduced epidermal cell "energy" in AQP3 deficiency, leading to reduced cell proliferation. The remarkable resistance to skin tumorigenesis in AQP3 deficiency provides a rational basis for evaluation of AQP3 inhibitors for prevention and therapy of skin and other tumors associated with AQP3 overexpression.

* Corresponding author. Mailing address: Cardiovascular Research Institute, 1246 Health Sciences East Tower, Box 0521, University of California—San Francisco, San Francisco, CA 94143-0521. Phone: (415) 476-8530. Fax: (415) 665-3847. E-mail: Alan.Verkman@ucsf.edu.

† Supplemental material for this article may be found at http://mcb.asm.org/.

▽ Published ahead of print on 29 October 2007.

MATERIALS AND METHODS

Mice. AQP3$^{-/-}$ mice (CD1 and SKH1 hairless genetic backgrounds) were generated by targeted gene disruption as described previously (16). Protocols were approved by the UCSF Committee on Animal Research.

Tumorigenesis model. Six- to 7-week-old AQP3$^{+/+}$ and AQP3$^{-/-}$ mice (CD1 and SKH1 backgrounds) were used. Dorsal hair samples of CD1 mice were removed by shaving at 2 days prior to treatment. A single application of DMBA

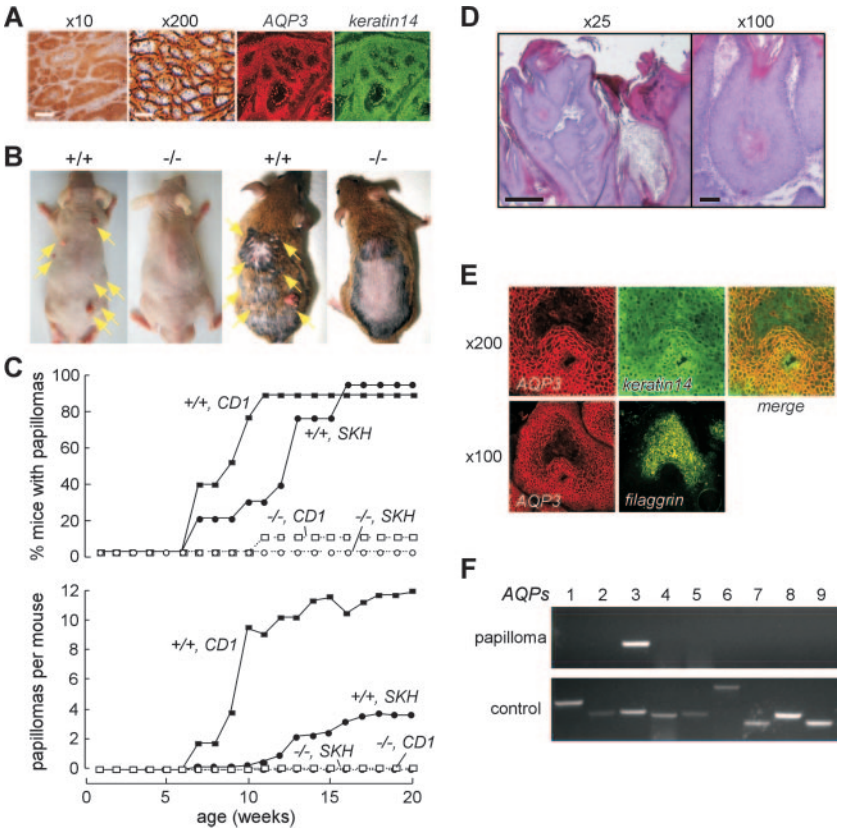

FIG. 1. AQP3 expression in human SCC and protection against cutaneous papillomas in AQP3-null mice. (A) (left) AQP3 immunostaining in human SCC (male, age 58 years). Bars, 200 μm (×10) and 20 μm (×200). (Right) Immunostaining of AQP3 and keratin-14 in SCC. (B) Dorsal skin of mice was treated with DMBA and TPA as described in Materials and Methods. Representative photographs showing multiple papillomas in AQP3$^{+/+}$ mice (left, SKH background; right, CD1) but no papillomas in AQP3$^{-/-}$ mice. (C) (top) Percentages of mice with papillomas. (Bottom) Average numbers of papillomas per mouse (9 to 12 mice per group). (D) Histology of papillomas stained with hematoxylin and eosin. Bars, 500 μm (×25) and 100 μm (×100). (E) Immunostaining of AQP3 and keratin-14 or filaggrin in papilloma of AQP3$^{+/+}$ mouse. (F) RT-PCR analysis of AQPs 1 to 9 in papilloma isolated from AQP3$^{+/+}$ mouse. Control amplifications were done using a mixture of cDNAs from brain, lung, liver, and kidney.

(25 nmol in 200 μl acetone) over ~12 cm^2 skin was given, followed by twice-weekly applications of TPA (6.8 nmol in 200 μl acetone) for 20 weeks. The number of papillomas was counted weekly.

Primary culture of mouse keratinocytes. Full-thickness skin samples from 1- to 3-day-old mice were incubated in dispase II (5 U/ml; Boehringer Mannheim) for 7 h at 4°C. The epidermis was separated from the dermis, cut into fragments, and incubated in 0.25% trypsin-0.1% EDTA for 10 min. Cells were seeded on collagen type I plates (BD Biosciences) at a density of 10^5 per cm^2 and cultured in keratinocyte growth medium (Cambrex Inc.) at 37°C under 5% CO_2.

RT-PCR. Total RNA was isolated from papillomas of AQP3$^{+/+}$ mice by using TRIzol (Invitrogen). Reverse transcription (RT)-PCR was performed using sequence-specific sense and antisense oligonucleotide primers for mouse AQPs 1 through 9, as described previously (16).

Epidermal cell proliferation, differentiation, and apoptosis. Dorsal skin was treated with one or four applications of TPA (6.8 nmol in 200 μl acetone) or vehicle, and skin was excised at 24 h after treatment. For measurement of epidermal cell proliferation, mice were injected intraperitoneally with BrdU (100 μg/g body weight; Sigma-Aldrich) at 1 h prior to sacrifice. Paraffin-embedded sections were stained with hematoxylin and eosin or anti-BrdU antibody (ABcam) with biotinylated anti-rat immunoglobulin G and horseradish peroxidase-conjugated ABC reagent (Vector Laboratories Inc.). Epidermal thickness was measured at 10 or more locations per mouse. The BrdU-positive cells among the >200 basal cells examined per mouse were counted. Epidermal cell differentiation was assessed following four TPA applications by immunostaining with filaggrin (CRP Inc.) and keratin-10 (Chemicon) antibodies. Apoptotic cells in the epidermis at 24 h after DMBA application (100 nmol in 200 μl acetone) were detected by terminal deoxynucleotidyltransferase-mediated dUTP-biotin nick end labeling (TUNEL) staining using an in situ cell death detection kit (Roche Applied Science). As a positive control, the epidermis was stained following DNase I treatment (2,000 U/ml, 10 min).

TPA penetration into the epidermis. Skin was excised at 30 min and 18 h after application of [20-^{3}H]TPA (150 μCi/mmol; American Radiolabeled Chemical). After removal of the stratum corneum by tape stripping, epidermal sheets were separated from the dermis by incubation at 60°C for 10 s and homogenized in lysis buffer (Cell Signaling Technology). ^{3}H radioactivity and protein content were measured in supernatant after homogenization and centrifugation at 1,000 rpm.

Glycerol incorporation into the epidermis and CO_2 production. Skin was excised at 16 h after TPA treatment, and 18-mm-diameter punch samples were incubated for 3 h in 1 ml of keratinocyte growth medium containing [^{14}C]glycerol (2 μCi/ml). Lipid and aqueous fractions were extracted from the epidermis, and ^{14}C radioactivity was measured as described previously (9). To measure $^{14}CO_2$ release, whole skin was incubated for 2 h in 1 ml of keratinocyte growth medium containing [^{14}C]glycerol (5 μCi/ml) in a 35-mm dish. Oxidation products were trapped on filter paper saturated with 2 M NaOH, as described previously (19), and $^{14}CO_2$ was quantified in 1-ml aliquots of the water wash.

Water and glycerol permeability. Water permeability was measured by calcein fluorescence quenching, as described previously (24). The change in calcein fluorescence following an increase in perfusate osmolality from 300 (phosphate-buffered saline [PBS]) to 600 (PBS containing 300 mM mannitol) mosM was monitored. Glycerol permeability was measured by [^{14}C]glycerol uptake at 3 min, as described previously (11).

Measurement of glycerol, glucose, ATP, and G3P content and ADP/ATP ratio. Supernatants of epidermal and cell homogenates (3,500 × *g*, 10 min, 4°C) were assayed for glycerol and glucose by using commercial kits (glycerol, Roche;

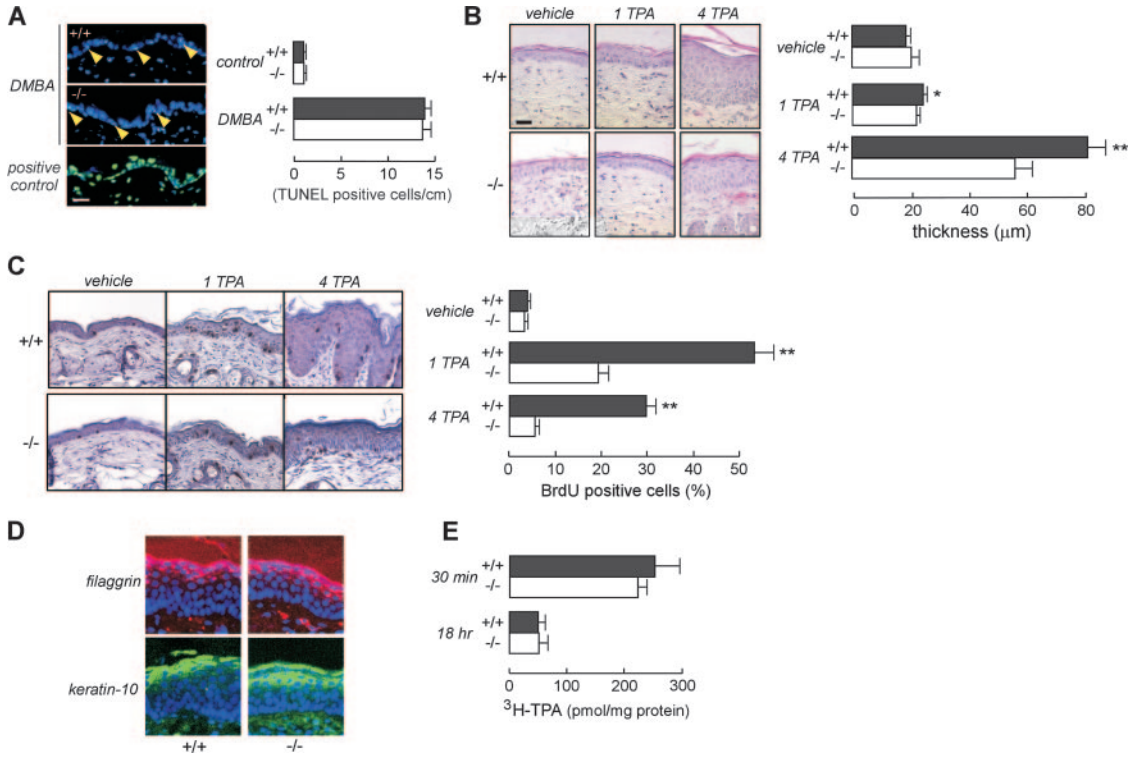

FIG. 2. Impaired epidermal cell proliferation in the AQP3$^{-/-}$ epidermis. (A) (left) TUNEL staining of an epidermis treated with DMBA. The positive control was DNase I treatment. Arrowhead, TUNEL-positive cell. Bar, 20 μm. (Right) Numbers of TUNEL-positive cells in the epidermis, within 1 cm (error bars indicate standard errors; $n = 4$). (B) (left) Hematoxylin and eosin staining of an epidermis treated topically with vehicle or one or four applications of TPA (1 TPA or 4 TPA). Bar, 20 μm. (Right) Epidermal thickness in AQP3$^{+/+}$ and AQP3$^{-/-}$ mice (error bars indicate standard errors; $n = 5$; asterisk, $P < 0.05$; two asterisks, $P < 0.01$). (C) (left) BrdU staining of the epidermis following treatment with vehicle or one or four TPA applications. (Right) Percentages of BrdU-positive cells in the epidermal basal layer (error bars indicate standard errors; $n = 4$; two asterisks, $P < 0.01$). (D) Immunostaining of filaggrin and keratin-10 in the epidermis after four TPA applications. Nuclei were stained with DAPI (4′,6′-diamidino-2-phenylindole) (blue). (E) [^{3}H]TPA penetration in the epidermis after a single application (error bars indicate standard errors; $n = 4$ or 5).

glucose, Sigma). ATP content was assayed using an ATP bioluminescence assay kit (Roche) according to manufacturer's instructions. Glycerol-3-phosphate (G3P) was measured spectrophotometrically as described before (21). ADP/ATP ratio was measured using an ApoSENSOR ADP/ATP ratio assay kit (BioVision).

ATP production assay. A mitochondrial fraction from AQP3$^{+/+}$ mouse epidermis was obtained as described previously (7). Mitochondrial ATP production was assayed as described previously (13).

Glycerol administration. Mice were provided ad libitum with water containing glycerol (5% for AQP3$^{+/+}$ mice and 1% for AQP3$^{-/-}$ mice) for 3 days prior to TPA treatment, along with standard solid mouse chow. BrdU was labeled at 23 h after TPA treatment.

Statistical analysis. Statistical analysis was performed with a two-tailed indirect Student t test or analysis of variance.

RESULTS

AQP3-deficient mice are resistant to development of skin tumors. To investigate the involvement of AQP3 in skin cancer, we examined AQP3 expression in human cutaneous SCC. Forty SCC samples from different human subjects were immunostained for AQP3. We found strong AQP3 expression in a plasma membrane pattern in every SCC sample (example in Fig. 1A). Colabeling with the basal cell marker keratin-14 showed AQP3 expression in basal cells in SCC (Fig. 1A, right).

To address the role of AQP3-mediated water/glycerol transport during skin tumor formation, we used a well-established multistage model of tumorigenesis that mimics human SCC (3, 14, 30). Dorsal skin of wild-type (AQP3$^{+/+}$) and AQP3-null (AQP3$^{-/-}$) mice was treated with a single dose of the tumor initiator DMBA, followed by multiple applications of the tumor promoter TPA. Figure 1B shows the development of multiple papillomas in AQP3$^{+/+}$ mice in both hairless (SKH1) and nonhairless (CD1) genetic backgrounds. Papillomas were absent in identically treated AQP3$^{-/-}$ mice. Figure 1C shows that AQP3$^{-/-}$ mice were remarkably resistant to the formation of skin tumors. Nearly all AQP3$^{+/+}$ mice developed papillomas by 15 weeks after DMBA/TPA treatment in both hairless SKH1 and CD1 genetic backgrounds (Fig. 1C), as expected from previous reports (3, 30). Figure 1D shows the histological appearance of papillomas in AQP3$^{+/+}$ mice. Immunostaining shows strong expression of AQP3 with a plasma membrane pattern in papilloma cells (Fig. 1E), similar to what was found for human SCC. AQP3 colocalized with keratin-14 but not with the differentiation marker filaggrin (Fig. 1E). RT-PCR screening for AQPs in mouse papillomas revealed only the expression of the AQP3 transcript (Fig. 1F).

Impaired TPA-induced cell proliferation in the AQP3-deficient epidermis. In the two-step carcinogenesis model, initial application of the chemical mutagen DMBA causes significant DNA damage, which results in apoptotic epidermal cell death

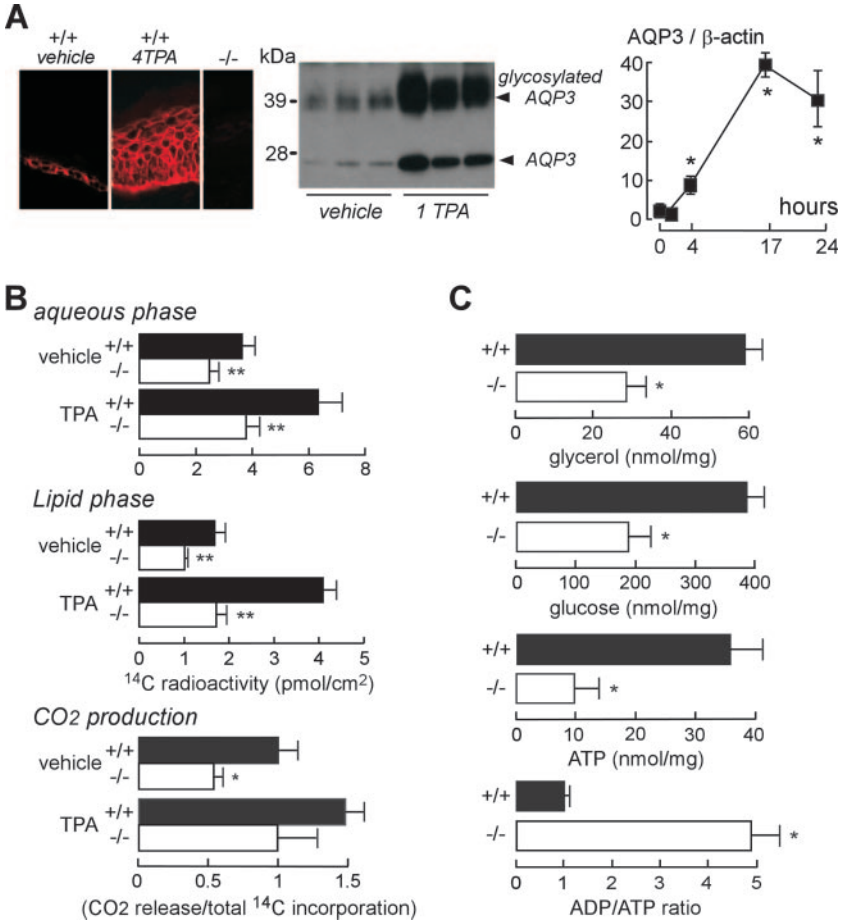

FIG. 3. Reduced cellular ATP content in the AQP3-deficient epidermis. (A) (left) AQP3 immunostaining of an epidermis treated with vehicle or four TPA applications (4 TPA). (Center) AQP3 immunoblot of the epidermis 24 h after one TPA application (1 TPA). (Right) Time course of AQP3 protein expression (as AQP3/β-actin ratios) (error bars indicate standard errors; $n = 3$ to 5; asterisk, $P < 0.01$). (B) [^{14}C]glycerol incorporation into epidermal aqueous (top) and lipid (middle) phases. (Bottom) $^{14}CO_2$ release from the epidermis, normalized to total ^{14}C incorporation. Measurements were done with organ cultured skin after 16 h of treatment with vehicle or TPA (error bars indicate standard errors; $n = 4$; two asterisks, $P < 0.01$; asterisk, $P < 0.05$). (C) Glycerol, glucose, and ATP content and ADP/ATP ratios in AQP3$^{+/+}$ and AQP3$^{-/-}$ epidermises (error bars indicate standard errors; $n = 5$; asterisk, $P < 0.01$).

and Ha-*ras* mutation (3, 14, 30). DMBA challenge produced comparable apoptotic responses in AQP3$^{-/-}$ and AQP3$^{+/+}$ epidermises (Fig. 2A), suggesting that AQP3 expression did not affect the tumor initiation step. Treatment with the tumor promoter TPA strongly induces cell proliferation, which is necessary for clonal expansion of initiated cells (3, 14, 30). Epidermal cell proliferation was measured following topical application of TPA once or daily for four days. Figure 2B shows greater hyperplasia after four TPA treatments in AQP3$^{+/+}$ than in AQP3$^{-/-}$ mice. Epidermal cell proliferation was much greater in AQP3$^{+/+}$ mice than in AQP3$^{-/-}$ mice, as shown by the greater percentage of BrdU-positive epidermal cells following TPA treatment (Fig. 2C). After four TPA treatments, epidermal cell proliferation in AQP3$^{-/-}$ mice returned to near the baseline, suggesting that TPA-induced continuous cell proliferation requires AQP3 expression (Fig. 2C, right).

Previous indirect evidence has suggested the involvement of AQP3 in keratinocyte differentiation (31), which might be involved in the tumor promotion step. However, we found comparable amounts of the differentiation markers filaggrin and keratin-10 in AQP3$^{+/+}$ and AQP3$^{-/-}$ epidermises, even after four TPA applications (Fig. 2D). Figure 2E shows comparable levels of TPA exposure in AQP3$^{+/+}$ and AQP3$^{-/-}$ mice as assessed by epidermis-associated [^{3}H]TPA radioactivity at 30 min and 18 h after exposure, ruling out the differences in tumor promoter exposure between the two groups. Together, these findings implicate AQP3 deficiency in the impaired TPA-induced cell proliferation during tumor promotion, which is responsible for the absence of papillomas.

Reduced cellular ATP in AQP3-deficient epidermal cells. To investigate the involvement of AQP3 in impaired TPA-induced proliferation, we measured the effect of TPA treatment on AQP3 expression. Epidermal cells from TPA-treated AQP3$^{+/+}$ mice strongly expressed AQP3 protein in a plasma membrane pattern (Fig. 3A, left). Figure 3A (right) shows significantly increased AQP3 protein expression, even at 4 h after TPA treatment. We reported previously that impaired AQP3-mediated glycerol transport was responsible for the dry skin and delayed barrier recovery in AQP3 deficiency (9, 10). To investigate the potential role of AQP3-facilitated glycerol transport

in TPA-induced proliferation, we measured [^{14}C]glycerol incorporation and CO_2 production. Figure 3B shows reduced [^{14}C]glycerol incorporation into the lipid and aqueous phases of the AQP3$^{-/-}$ epidermis following TPA treatment. Reduced conversion of [^{14}C]glycerol into $^{14}CO_2$ was also found in the AQP3$^{-/-}$ epidermis (Fig. 3B, bottom panel). There was little difference in lipid amount between membrane-rich fractions of epidermal cells from AQP3$^{+/+}$ and AQP3$^{-/-}$ mice, except for a small reduction in free fatty acids and cholesterol sulfate (see Fig. S1 in the supplemental material); however, this reduction is unlikely to account for differences in epidermal cell proliferation and papilloma formation. Also, analysis of epidermal cell plasma membrane fluidity by fluorescence recovery after photobleaching showed no significant differences in AQP3$^{-/-}$ deficiency (data not shown).

We therefore focused on aqueous-phase glycerol metabolism. Figure 3C shows significantly reduced epidermal glycerol, glucose, and ATP content, indicating that the absence of AQP3 results in impaired cellular metabolism. Epidermal cell ADP/ATP ratios were remarkably increased, indicating altered cellular energy balance in AQP3$^{-/-}$ epidermal cells. The data in Fig. 3C suggested an unexpected role for AQP3 in epidermal cell ATP generation.

We verified this phenomenon in primary keratinocyte cell cultures from mice. Figure 4A and B shows decreased water and glycerol transport in AQP3-deficient keratinocyte cultures. Reduced cellular glycerol, glucose, ATP, and CO_2 production was also found in AQP3-deficient keratinocytes (Fig. 4C). We also confirmed the involvement of AQP3 in cellular ATP in normal human keratinocytes. AQP3 knock-down in normal human keratinocytes by small interfering RNA-AQP3 reduced AQP3 protein expression by ~95% and decreased water permeability and glycerol uptake (see Fig. S2A to C in the supplemental material). Reduced glycerol and ATP content was found in the AQP3 knock-down keratinocytes (see Fig. S2D and E in the supplemental material).

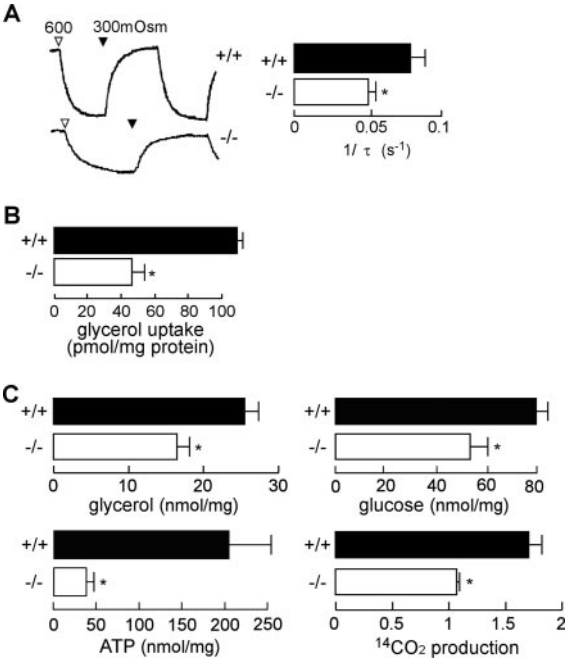

FIG. 4. Decreased cellular ATP content in AQP3-deficient mouse keratinocytes. Keratinocytes were cultured from AQP3$^{+/+}$ and AQP3$^{-/-}$ mouse epidermis. (A) (left) Osmotic water permeability as measured by calcein fluorescence quenching. The change in calcein fluorescence following an increase in perfusate osmolality from 300 (PBS) to 600 (PBS containing 300 mM mannitol) mosM was monitored. (Right) Reciprocal exponential time constants (τ^{-1}, proportional to osmotic water permeability) in five separate sets of measurements (error bars indicate standard errors; $n = 5$; asterisk, $P < 0.01$). (B) Glycerol permeability as measured by [^{14}C]glycerol uptake for 3 min (error bars indicate standard errors; $n = 5$, asterisk, $P < 0.01$). (C) Glycerol, glucose, and ATP content in AQP3$^{+/+}$ and AQP3$^{-/-}$ keratinocytes. $^{14}CO_2$ release from keratinocytes, normalized to total ^{14}C incorporation (error bars indicate standard errors; $n = 5$; asterisk, $P < 0.01$).

Involvement of AQP3-mediated glycerol uptake in cellular ATP generation and proliferation. We postulated that AQP3-mediated glycerol transport is involved in cellular ATP generation, which provides the energy for cell proliferation and tumor formation. To test this idea, we measured intracellular ATP content in primary cultures of keratinocytes incubated with glycerol for 1 day. Figure 5A shows that glycerol supplementation increased intracellular ATP content in a dose-dependent manner, with a lesser increase in AQP3-deficient keratinocytes. Of note, glycerol can be transported into cells both through the lipid bilayer and by AQP3 (10, 16). The metabolic inhibitor 2-deoxyglucose (2-dOG) reduced ATP content. Figure 5B shows a positive correlation between cellular glycerol and ATP content in AQP3$^{+/+}$ keratinocytes under a variety of conditions (different external glycerol, absence or presence of 2-dOG, wild-type versus AQP3-deficient cells), supporting the involvement of AQP3-mediated glycerol transport in intracellular ATP generation.

To investigate the potential importance of AQP3-dependent glycerol accumulation in epidermal ATP generation, we measured G3P, which is produced from glycerol and is an important metabolic intermediate for energy metabolism in the mitochondria (2, 17). G3P content was significantly reduced in the AQP3$^{-/-}$ epidermis, supporting the involvement of AQP3-mediated glycerol uptake in G3P production (Fig. 5C). We then examined whether G3P could produce ATP in a mitochondrion-rich fraction from the epidermis. Figure 5D shows that G3P, but not glycerol, induced ATP generation. ATP production rates were comparable in AQP3$^{+/+}$ and AQP3$^{-/-}$ mitochondria, suggesting that AQP3 deficiency does not interfere with intrinsic mitochondrial function (Fig. 5E).

We next tested whether AQP3-dependent cellular ATP generation could be the critical determinant in epidermal proliferation. BrdU incorporation and ATP content in AQP3$^{+/+}$ and AQP3$^{-/-}$ keratinocytes were assayed after treatment with glycerol or 2-dOG. Figure 5F shows a positive correlation between cell proliferation and ATP content. These results support a mechanism for epidermal cell proliferation involving AQP3-dependent cell glycerol content as an important determinant of ATP content and cell proliferation.

We tested whether glycerol supplementation could correct the impaired cell proliferation in AQP3 deficiency. Mice were given glycerol orally for 3 days prior to TPA treatment, which corrects the glycerol content in the AQP3$^{-/-}$ epidermis (10). Figure 6 shows that glycerol administration corrected the impaired epidermal proliferative response, as seen from

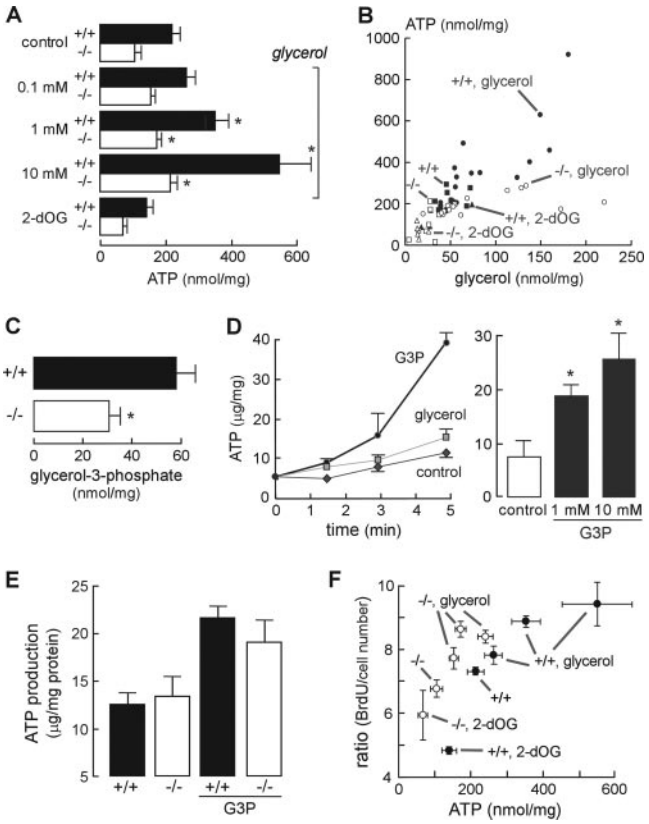

FIG. 5. Involvement of AQP3-mediated glycerol uptake in ATP generation and cell proliferation. (A) Intracellular ATP content in cultured AQP3$^{+/+}$ and AQP3$^{-/-}$ keratinocytes incubated with glycerol (0.1, 1, or 10 mM, 24 h) or 2-dOG (5 mM, 1 h) (error bars indicate standard errors; $n = 5$; asterisk, $P < 0.05$ for comparison with control). (B) Correlation between cellular glycerol and ATP content in cultured AQP3$^{+/+}$ and AQP3$^{-/-}$ keratinocytes. (C) G3P content in AQP3$^{+/+}$ and AQP3$^{-/-}$ epidermis (error bars indicate standard errors; $n = 5$; asterisk, $P < 0.01$). (D) G3P-induced ATP production in a mitochondrial fraction from an AQP3$^{+/+}$ epidermis. (Left) ATP content in the mitochondrion-rich fraction incubated with G3P or glycerol (10 mM). (Right) ATP production in the mitochondrial fraction after incubation with 1 or 10 mM G3P for 5 min (error bars indicate standard errors; $n = 5$; asterisk, $P < 0.01$). (E) ATP production in the mitochondrial fractions from AQP3$^{+/+}$ and AQP3$^{-/-}$ epidermis incubated with 10 mM G3P (error bars indicate standard errors; $n = 5$). (F) Correlation between cellular ATP content and cell proliferation as detected by a BrdU enzyme-linked immunosorbent assay. Ratios are expressed as BrdU incorporation per cell number.

measurements of percentage of BrdU-positive cells. This result provides strong evidence for AQP3-facilitated glycerol transport as an important determinant of epidermal cell proliferation.

DISCUSSION

The principal finding here is the remarkable resistance of AQP3-deficient mice to the development of skin tumors. Impaired TPA-mediated proliferation was seen in the AQP3-deficient epidermis during the tumor promotion step. Epidermal differentiation, TPA exposure, and DMBA sensitivity were comparable in wild-type and AQP3-deficient epidermises and thus not responsible for absence of papillomas in AQP3-null

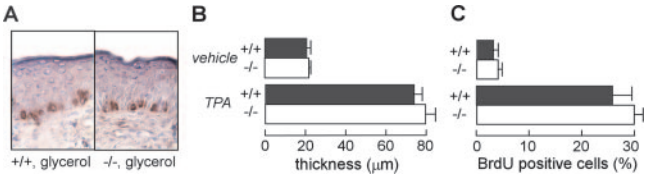

FIG. 6. Glycerol administration corrects impaired proliferation in the AQP3$^{-/-}$ mouse epidermis. Mice were administrated glycerol orally for 3 days prior to TPA treatment. (A) BrdU staining of the epidermis at 24 h after TPA treatment. (B and C) Epidermal thickness (B) and percentages of BrdU-positive cells (C) in the basal epidermal layer (error bars indicate standard errors; $n = 4$).

mice. We postulated that impaired cell proliferation is responsible for the lack of promotion of the initiated cells, resulting in the absence of papillomas. Analysis of mechanism indicated markedly reduced intracellular ATP content as well as reduced glycerol and glucose content in AQP3-deficient keratinocytes. Glycerol supplementation increased intracellular ATP in AQP3$^{+/+}$ keratinocytes, with a lesser increase in AQP3-deficient keratinocytes. We found a positive correlation between glycerol and ATP content in AQP3$^{+/+}$ keratinocytes, suggesting the involvement of AQP3-mediated glycerol transport in ATP generation. Also, cell proliferation correlated with ATP content. Together, these data provide evidence for the involvement of AQP3-facilitated glycerol transport in ATP generation and regulation of epidermal cell proliferation.

Although ATP is thought to be the major energy source in the epidermis as well as in tumor formation (6, 8, 17, 18, 23), the detailed metabolic pathways of ATP production/synthesis in the epidermis have not been established, nor has the role of glycerol metabolism, which is quite tissue specific (2). Glycerol kinase, which catalyzes the phosphorylation of glycerol to yield G3P, is strongly expressed in liver and kidney but is less active in intestinal mucosa, adipocytes, and skeletal muscle (2). In humans, about 60% of synthesized glycerol is converted into G3P as a key metabolic intermediate in ATP production (1, 2, 17). Our data suggest the involvement of AQP3-facilitated glycerol cellular uptake in epidermal G3P production and ATP generation. Further, we conclude that AQP3-facilitated glycerol transport is required to maintain high levels of intracellular glycerol for ATP generation, which may be important in states of epidermal hyperproliferation, such as psoriasis, ichthyosis, atopic dermatitis, wound healing, and tumorigenesis.

Tumor-committed cells generally have an aggressive energy metabolic profile. Changes in cell metabolism occur early in tumor cell development, providing increased energy for cell growth and tumor formation (6, 17, 18). Our data suggest the requirement of AQP3-facilitated glycerol transport in epidermal cell proliferation and tumorigenesis promoted by a novel mechanism in which cellular glycerol is a key regulator of cellular ATP energy. We propose AQP3-facilitated glycerol transport to be of central importance in generating ATP, which facilitates the growth and survival of tumor cells (Fig. 7). Our data provide the first evidence for involvement of an AQP in cell energy metabolism. AQP3 may be also an important determinant in tumorigenesis of other tissues where AQP3 is expressed, including kidney, airway, urinary bladder, corneal (15), and intestinal (26) tissues. Our results suggest the possi-

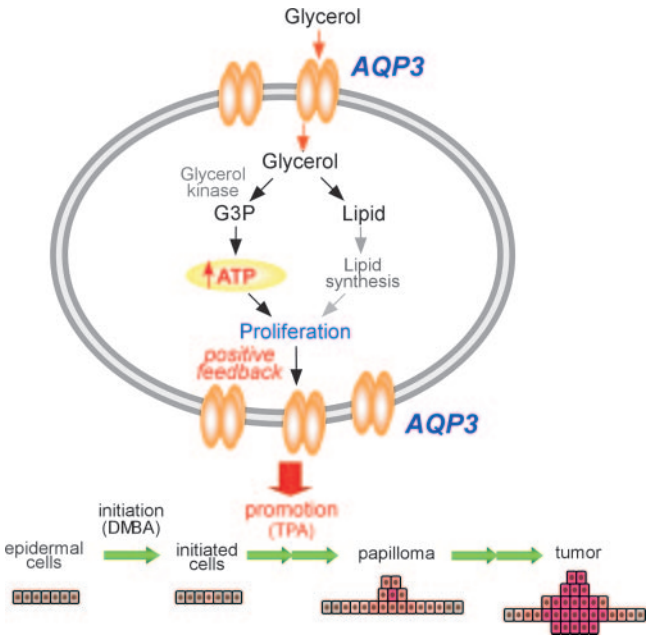

FIG. 7. Proposed mechanism of tumor promotion by AQP3-dependent cell proliferation during skin tumorigenesis.

bility of AQP3 inhibition or down-regulation in the prevention and therapy of skin and possibly other tumors.

ACKNOWLEDGMENTS

This work was funded by grants DK35124, HL73856, HL59198, EB00415, EY13574, and DK72517 from the National Institutes of Health and Research Development Program and Drug Discovery grants from the Cystic Fibrosis Foundation.

We thank Liman Qian for mouse breeding and genotype analysis, Tonghui Ma for help with RT-PCR analysis, and Shunsuke Chikuma for helpful discussions.

REFERENCES

1. **Baba, H., X. J. Zhang, and R. R. Wolfe.** 1995. Glycerol gluconeogenesis in fasting humans. Nutrition **11:**149–153.
2. **Brisson, D., M. C. Vohl, J. St-Pierre, T. J. Hudson, and D. Gaudet.** 2001. Glycerol: a neglected variable in metabolic processes? Bioessays **23:**534–542.
3. **DiGiovanni, J.** 1992. Multistage carcinogenesis in mouse skin. Pharmacol. Ther. **54:**63–128.
4. **Frigeri, A. M., A. Gropper, F. Umenishi, M. Kawashima, D. Brown, and A. S. Verkman.** 1995. Localization of MIWC and GLIP water channel homologs in neuromuscular, epithelial and glandular tissues. J. Cell Sci. **108:**2993–3002.
5. **Fujiyoshi, Y., K. Mitsuoka, B. L. de Groot, A. Philippsen, H. Grubmuller, P. Agre, and A. Engel.** 2002. Structure and function of water channels. Curr. Opin. Struct. Biol. **12:**509–515.
6. **Gatenby, R. A., and R. J. Gillies.** 2004. Why do cancers have high aerobic glycolysis? Nat. Rev. Cancer **4:**891–899.
7. **Gonzalez Maglio, D. H., M. L. Paz, A. Ferrari, F. S. Weill, A. Czerniczyniec, J. Leoni, and J. Bustamante.** 2005. Skin damage and mitochondrial dysfunction after acute ultraviolet B irradiation: relationship with nitric oxide production. Photodermatol. Photoimmunol. Photomed. **21:**311–317.
8. **Hammar, H.** 1976. Studies on the carbohydrate metabolism in psoriatic epidermis. Ann. Clin. Res. **8:**323–334.
9. **Hara, M., T. Ma, and A. S. Verkman.** 2002. Selectively reduced glycerol in skin of aquaporin-3-deficient mice may account for impaired skin hydration, elasticity, and barrier recovery. J. Biol. Chem. **277:**46616–46621.
10. **Hara, M., and A. S. Verkman.** 2003. Glycerol replacement corrects defective skin hydration, elasticity, and barrier function in aquaporin-3-deficient mice. Proc. Natl. Acad. Sci. USA **100:**7360–7365.
11. **Hara-Chikuma, M., E. Sohara, T. Rai, M. Ikawa, M. Okabe, S. Sasaki, S. Uchida, and A. S. Verkman.** 2005. Progressive adipocyte hypertrophy in aquaporin-7-deficient mice: adipocyte glycerol permeability as a novel regulator of fat accumulation. J. Biol. Chem. **280:**15493–15496.
12. **Hibuse, T., N. Maeda, T. Funahashi, K. Yamamoto, A. Nagasawa, W. Mizunoya, K. Kishida, K. Inoue, H. Kuriyama, T. Nakamura, T. Fushiki, S. Kihara, and I. Shimomura.** 2005. Aquaporin 7 deficiency is associated with development of obesity through activation of adipose glycerol kinase. Proc. Natl. Acad. Sci. USA **102:**10993–10998.
13. **Idahl, L. A., and N. Lembert.** 1995. Glycerol 3-phosphate-induced ATP production in intact mitochondria from pancreatic B-cells. Biochem. J. **15:** 287–292.
14. **Kemp, C. J.** 2005. Multistep skin cancer in mice as a model to study the evolution of cancer cells. Semin. Cancer Biol. **15:**460–473.
15. **Levin, M. H., and A. S. Verkman.** 2006. Aquaporin-3-dependent cell migration and proliferation during corneal re-epithelialization. Investig. Ophthalmol. Vis. Sci. **47:**4365–4372.
16. **Ma, T., M. Hara, R. Sougrat, J. M. Verbavatz, and A. S. Verkman.** 2002. Impaired stratum corneum hydration in mice lacking epidermal water channel aquaporin-3. J. Biol. Chem. **277:**17147–17153.
17. **Mazurek, S., C. B. Boschek, and E. Eigenbrodt.** 1997. The role of phosphometabolites in cell proliferation, energy metabolism, and tumor therapy. J. Bioenerg. Biomembr. **29:**315–330.
18. **Moreno-Sanchez, R., S. Rodriguez-Enriquez, A. Marin-Hernandez, and E. Saavedra.** 2007. Energy metabolism in tumor cells. FEBS J. **274:**1393–1418.
19. **Muoio, D. M., K. Seefeld, L. A. Witters, and R. A. Coleman.** 1999. AMP-activated kinase reciprocally regulates triacylglycerol synthesis and fatty acid oxidation in liver and muscle: evidence that sn-glycerol-3-phosphate acyltransferase is a novel target. Biochem. J. **338:**783–791.
20. **Nakakoshi, M., Y. Morishita, K. Usui, M. Ohtsuki, and K. Ishibashi.** 2006. Identification of a keratinocarcinoma cell line expressing AQP3. Biol. Cell **98:**95–100.
21. **Reithmann, C., C. Scheininger, T. Bulgan, and K. Werdan.** 1996. Exposure to the n-3 polyunsaturated fatty acid docosahexaenoic acid impairs alpha 1-adrenoceptor-mediated contractile responses and inositol phosphate formation in rat cardiomyocytes. Naunyn Schmiedebergs Arch. Pharmacol. **354:**109–119.
22. **Rojek, A. M., M. T. Skowronski, E. M. Fuchtbauer, A. C. Fuchtbauer, R. A. Fenton, P. Agre, J. Frokiaer, and S. Nielsen.** 2007. Defective glycerol metabolism in aquaporin 9 (AQP9) knockout mice. Proc. Natl. Acad. Sci. USA **104:**3609–3614.
23. **Ronquist, G., A. Andersson, N. Bendsoe, and B. Falck.** 2003. Human epidermal energy metabolism is functionally anaerobic. Exp. Dermatol. **12:**572–579.
24. **Saadoun, S., M. C. Papadopoulos, M. Hara-Chikuma, and A. S. Verkman.** 2005. Impairment of angiogenesis and cell migration by targeted aquaporin-1 gene disruption. Nature **434:**786–792.
25. **Sougrat, R., M. Morand, C. Gondran, P. Barre, R. Gobin, F. Bonte, M. Dumas, and J. M. Verbavatz.** 2002. Functional expression of AQP3 in human skin epidermis and reconstructed epidermis. J. Investig. Dermatol. **118:**678–685.
26. **Thiagarajah, J. R., and A. S. Verkman.** 2007. Impaired enterocyte proliferation in aquaporin-3 deficiency in mouse models of colitis. Gut **56:**1529–1535.
27. **Verkman, A. S., and A. K. Mitra.** 2000. Structure and function of aquaporin water channels. Am. J. Physiol. Renal Physiol. **278:**F13–F28.
28. **Verkman, A. S.** 2005. Novel roles of aquaporins revealed by phenotype analysis of knockout mice. Rev. Physiol. Biochem. Pharmacol. **155:**31–55.
29. **Wu, X., and P. P. Pandolfi.** 2001. Mouse models for multistep tumorigenesis. Trends Cell Biol. **11:**S2–S9.
30. **Yuspa, S. H., and M. C. Poirier.** 1988. Chemical carcinogenesis: from animal models to molecular models in one decade. Adv. Cancer Res. **50:**25–70.
31. **Zheng, X., and W. B. Bollag.** 2003. Aquaporin 3 colocates with phospholipase d2 in caveolin-rich membrane microdomains and is downregulated upon keratinocyte differentiation. J. Investig. Dermatol. **121:**1487–1495.